Role for miR-204 in human pulmonary arterial hypertension

Audrey Courboulin,[1] Roxane Paulin,[1] Nellie J. Giguère,[2] Nehmé Saksouk,[2] Tanya Perreault,[1] Jolyane Meloche,[1] Eric R. Paquet,[1] Sabrina Biardel,[3] Steeve Provencher,[3] Jacques Côté,[2] Martin J. Simard,[2] and Sébastien Bonnet[1]

[1]Département de médecine, Faculté de médecine, [2]Centre de recherche en cancérologie de l'Université Laval, Hôtel-Dieu de Québec, and [3]Institut universitaire de cardiologie et de pneumologie de Québec, Université Laval, Québec, Québec G1V 0A6, Canada

Pulmonary arterial hypertension (PAH) is characterized by enhanced proliferation and reduced apoptosis of pulmonary artery smooth muscle cells (PASMCs). Because microRNAs have been recently implicated in the regulation of cell proliferation and apoptosis, we hypothesized that these regulatory molecules might be implicated in the etiology of PAH. In this study, we show that miR-204 expression in PASMCs is down-regulated in both human and rodent PAH. miR-204 down-regulation correlates with PAH severity and accounts for the proliferative and antiapoptotic phenotypes of PAH-PASMCs. STAT3 activation suppresses miR-204 expression, and miR-204 directly targets SHP2 expression, thereby SHP2 up-regulation, by miR-204 down-regulation, activates the Src kinase and nuclear factor of activated T cells (NFAT). STAT3 also directly induces NFATc2 expression. NFAT and SHP2 were needed to sustain PAH-PASMC proliferation and resistance to apoptosis. Finally, delivery of synthetic miR-204 to the lungs of animals with PAH significantly reduced disease severity. This study uncovers a new regulatory pathway involving miR-204 that is critical to the etiology of PAH and indicates that reestablishing miR-204 expression should be explored as a potential new therapy for this disease.

CORRESPONDENCE
Sébastien Bonnet:
sebastien.bonnet@crhdq.ulaval.ca

Abbreviations used: ChIP, chromatin immunoprecipitation; iPAH, idiopathic PAH; MCT, monocrotaline; miRNA, microRNA; mRNA, messenger RNA; NFAT, nuclear factor of activated T cells; PA, pulmonary artery; PAAT, PA acceleration time; PAEC, PA endothelial cell; PAH, pulmonary arterial hypertension; PASMC, PA smooth muscle cell; PCNA, proliferating cell nuclear antigen; PDGF, platelet-derived growth factor; qRT-PCR, quantitative RT-PCR; ROCK, Rho-associated, coiled-coil–containing protein kinase; seq, sequencing; siRNA, small interfering RNA; TLDA, TaqMan low density array; TMRM, tetramethylrhodamine methyl ester; TUNEL, terminal deoxynucleotidyl transferase dUTP nick end labeling; UTR, untranslated region; VEGF, vascular endothelial growth factor.

Pulmonary arterial hypertension (PAH) is a vascular disease that is largely restricted to small pulmonary arteries (PAs). PAH occurs in rare idiopathic and familial forms, but is more commonly part of a syndrome associated with connective tissue diseases, anorexigen use, HIV, or congenital heart disease. Many abnormalities contribute to this syndrome of obstructed, constricted small PAs. This includes abnormalities in the blood content of some neurotransmitters and cytokines, namely increases in serotonin, IL-6, platelet-derived growth factor (PDGF), and endothelin (Stewart et al., 1991; Christman et al., 1992; Steudel et al., 1997; Perros et al., 2008). The media is also characterized by an increased activation of the nuclear factor of activated T cells (NFAT), leading to increased $[Ca^{2+}]_i$-mediated PA smooth muscle cell (PASMC) proliferation and decreased mitochondrial-dependent apoptosis (Bonnet et al., 2006, 2007b). Finally, the adventitia is infiltrated with inflammatory cells and exhibits metalloprotease activation (Humbert et al., 2004). Despite recent therapeutic advances such as endothelin-1 receptor blockers (e.g., Bosentan; Dupuis and Hoeper, 2008), type 5 phosphodiesterase inhibitors (e.g., sildenafil; Li et al., 2007), or PDGF receptor blockers (e.g., imatinib; Ghofrani et al., 2005), mortality rates remain high (Archer and Rich, 2000). Moreover, the fact that the PAH phenotype is preserved in cultured PASMCs isolated from PAH patients suggests that the PAH phenotype is sustained independently of the circulating growth factors or agonists but requires genetic remodeling processes (Yildiz, 2009; Dumas de la Roque et al., 2010). Over the past 10 yr, genetic research on PAH has led to the discovery of mutations in the *BMPR2* (*bone morphogenetic receptor-2*) gene in at least 50% of familial PAH patients, and its down-regulation is recognized as a hallmark of PAH (Tada et al., 2007; Zakrzewicz et al., 2007). Recently, BMPR2 down-regulation in human

The Rockefeller University Press $30.00
J. Exp. Med. Vol. 208 No. 3 535-548
www.jem.org/cgi/doi/10.1084/jem.20101812

PASMCs has been linked to the activation of both the tyrosine kinase Src (Wong et al., 2005) and a STAT3/miR-17-92 microRNA (miRNA) secondary to IL-6 exposure, suggesting the implication of miRNAs in the etiology of PAH (Brock et al., 2009).

miRNAs are small noncoding RNAs (21–23 nt) that are now known to be important regulators of gene expression. They form imperfect RNA–RNA duplexes and use their seed region to interact with messenger RNAs (mRNAs), mainly in the 3′ untranslated region (UTR; Khan et al., 2009). This interaction leads to a negative posttranscriptional regulation of the relevant mRNAs. Recently, misexpression of miRNAs has been implicated in many cardiovascular diseases, including pulmonary hypertension (Latronico and Condorelli, 2009; Mishra et al., 2009; Zhang, 2009; Caruso et al., 2010), but their molecular role in these pathologies has not been uncovered yet.

RESULTS

miR-204 is aberrantly expressed in human PAH-PASMCs

To determine whether miRNAs are aberrantly expressed in human PAH, PASMCs were isolated from distal PAs of two nonfamilial PAH patients (two idiopathic PAH [iPAH] patients A and B; based on the World Health Organization [WHO] classification) and two control patients (A and B) and cultured as previously described (passage 3 and less; McMurtry et al., 2005). The expression of 377 different miRNAs was measured. Seven miRNAs were aberrantly expressed in PAH-PASMCs compared with control PASMCs (miR-204, -450a, -145, -302b, -27b, -367, and -138; Fig. S1 A). Among them, only the miR-204 level was down-regulated (Fig. S1 A). miR-204 down-regulation between control versus PAH was confirmed by quantitative RT-PCR (qRT-PCR) in PASMCs isolated from three PAH (all from group 1 based on WHO classification patients A–C) compared with control PASMCs isolated from five control patients (A–E). Note that no significant differences in miR-204 expression was found among the control patients and the PAH patients (Fig. S1 B). Therefore, for the rest of the study, all five control PASMC and the three PAH-PASMC cell lines were used for every cell-based experiment.

Interestingly, in retinal epithelial cells and several cancer cells, miR-204 down-regulation has been associated with enhanced cell proliferation and membrane potential depolarization (Lee et al., 2010; Wang et al., 2010), which are both aspects also seen in PAH-PASMCs (Bonnet et al., 2006, 2007b). We recently showed in several cancer cells and PAH-PASMCs (Bonnet et al., 2007a,b) that this pro-proliferative phenotype was associated in part with the activation of the Src–STAT3 (accounting for BMPR2 down-regulation; Wong et al., 2005) and NFAT pathways (Bonnet et al., 2007b). This suggests a putative link between miR-204 down-regulation, NFAT activation, and cell proliferation. Thus, miR-204 is likely implicated in PAH, and a role in the sustainability of the PAH-PASMC pro-proliferative and antiapoptotic phenotype is possible. Therefore, the current study will be focused on the role of miR-204 in the etiology of PAH. Interestingly, using in silico and microarray gene expression analyses, we observed that among the 461 predicted targets of miR-204 (TargetScan 5.1), only 165 were increased by artificial miR-204 inhibition in control human PASMCs ($n = 2$ patients; Fig. S1 C). In accordance with the pro-proliferative and antiapoptotic phenotypes seen in PAH, several Src–STAT3- and NFAT-related genes were identified (Fig. S1 C).

miR-204 expression is decreased in human PAH and correlates with PAH severity

To investigate the expression pattern of miR-204 in normal and pulmonary hypertensive lungs, we examined miR-204 expression levels in (a) lung biopsies from 8 individuals with nonfamilial PAH compared with biopsies from 8 individuals without pulmonary hypertension, (b) lungs from 6 mice with hypoxia-induced pulmonary hypertension compared with 5 control littermates, and (c) lungs from 5 rats with monocrotaline (MCT)-induced pulmonary hypertension compared with 10 control littermates (Fig. 1 A). We found decreased levels of miR-204 in human and rodent pulmonary hypertensive lung tissues compared with normotensive lung samples. To characterize whether down-regulated miR-204 levels were specific to the lung in rats with pulmonary hypertension, we compared organ-specific levels of miR-204 between normal and pulmonary hypertensive rats (Fig. 1 B). Even if we were able to detect minimal amounts of miR-204 in most organs, miR-204 levels were only down-regulated in the lung and PAs but not in the aorta, liver, heart, and kidney in rats 3 wk after MCT injection (pulmonary hypertensive rats) compared with non–pulmonary hypertensive rats (Fig. 1 B).

To test whether miR-204 down-regulation correlated with disease progression, we studied humans, mice, and rats with varying degrees of PAH. In both human subjects and rodents, miR-204 levels in the lung correlated directly with the severity of PAH, as measured by pulmonary vascular resistance in humans and mean PA pressure in rodents (Fig. 1 C). Our results indicate that levels of miR-204 correlate with the severity of PAH in humans and experimental pulmonary hypertension.

miR-204 is confined to PASMCs in the lung

To determine the lung distribution of miR-204, miR-204 expression was measured by qRT-PCR in rat bronchi, veins, and PAs. Our results indicate that miR-204 is in majority expressed within PAs but not in veins or bronchi tissue (Fig. S2 A). To determine the cell type distribution of miR-204 within PAs, miR-204 expression was measured in both cultured (passage 3 and less) human PASMCs and PA endothelial cells (PAECs). Our results indicate that within PAs, miR-204 is mostly confined to the PASMCs as control-cultured PASMCs expressed seven times more miR-204 compared with control PAECs (Fig. S2 B).

miR-204 expression level is a potent biomarker for PAH

Finally, because miRNAs are currently used in humans as a biomarker of cancer (Ferracin et al., 2010), to further

confirm the implication of miR-204 in PAH, we measured miR-204 expression level in human buffy coat isolated from non–pulmonary hypertensive patients and patients with PAH (Table S1). We previously showed that human PAH-PASMCs and cells from the buffy coat of PAH patients have a lot of similarities in term of activated pathways. For example, both have activated NFAT (Bonnet et al., 2007b); thus, miR-204 expression in the buffy coat could parallel miR-204 expression in PASMCs. Indeed, as in PAH-PASMCs, miR-204 expression was significantly decreased in patients with PAH (Fig. S2 C). This result is of a great clinical interest as it confirms the implication of miR-204 in PAH and suggests that miR-204 can become a reliable biomarker of PAH.

Diminution of miR-204 level promotes PASMC proliferation and resistance to apoptosis

To study the effect of miR-204 on PASMC proliferation and apoptosis in vitro, cultured human PAH-PASMCs were either exposed to 10% FBS to promote proliferation or 0.1% FBS to promote apoptosis (Bonnet et al., 2007b). When compared with control PASMCs containing a high level of miR-204, PAH-PASMCs displayed a higher cell proliferation rate and resistance to induced apoptosis (Fig. 2 A). The implication of miR-204 in regulating PASMC proliferation and apoptosis was confirmed in control PASMCs, in which miR-204 inhibition increased proliferation and resistance to apoptosis to levels similar to those seen in PAH-PASMCs (Fig. 2 A).

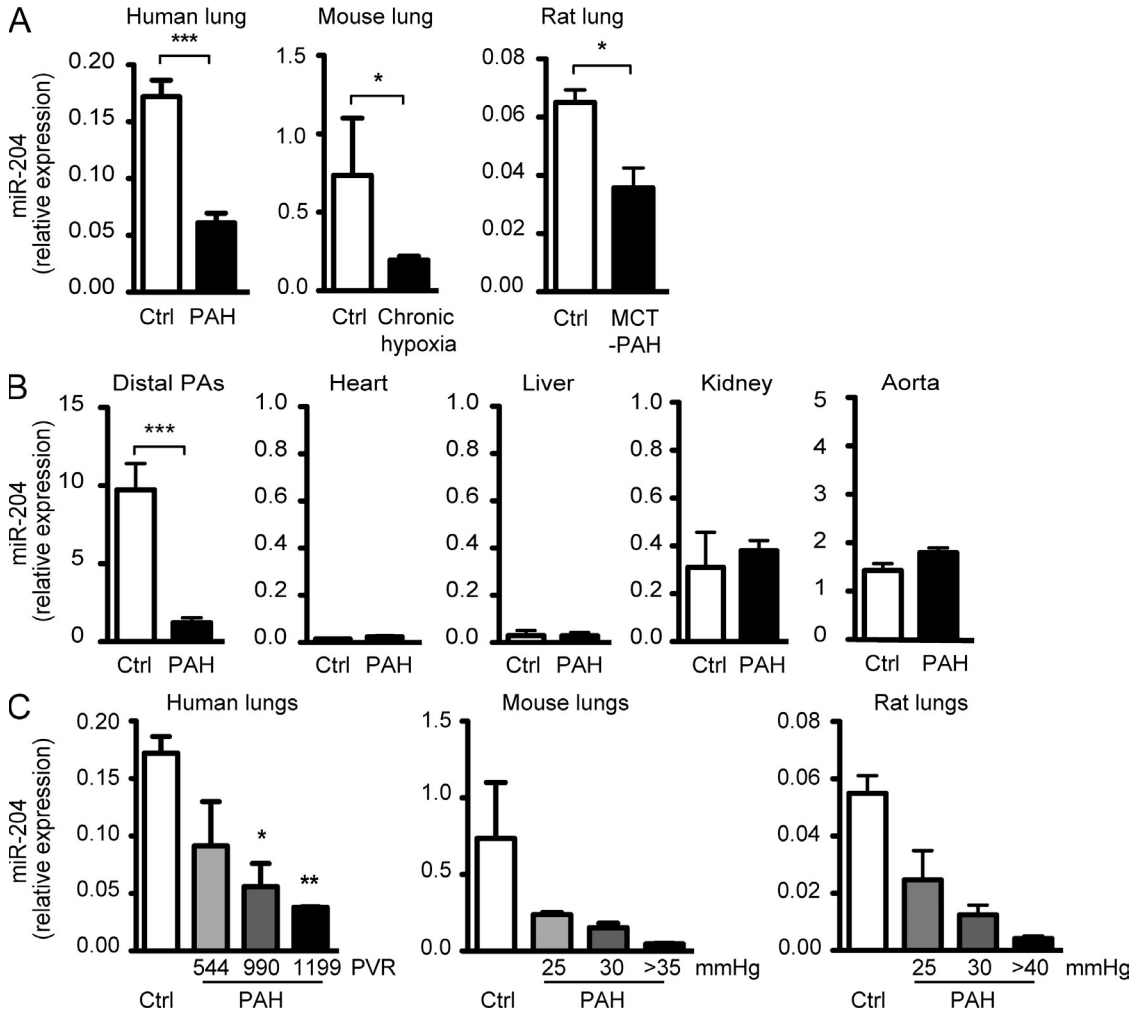

Figure 1. Correlation between miR-204 expression and PAH severity. (A) miR-204 is decreased in human, mouse, and rat PAH lungs. qRT-PCR analysis of miR-204 expression in human lungs with PAH ($n = 8$), mouse lungs with hypoxia-induced pulmonary hypertension ($n = 6$), and rat lungs with MCT-induced pulmonary hypertension ($n = 5$) compared with human ($n = 8$), mouse ($n = 10$) and rat ($n = 5$) control (Ctrl) lungs. (B) miR-204 is mainly expressed in the distal PAs. qRT-PCR analysis of miR-204 expression in several rat organs with MCT-induced pulmonary hypertension ($n = 5$) compared with control rats ($n = 5$). (C) miR-204 down-regulation correlates with PAH severity. qRT-PCR analysis of miR-204 expression in the lungs from healthy subjects ($n = 8$) and from patients with varying severity of PAH ($n = 3$), in mouse lungs with varying severity of hypoxia-induced pulmonary hypertension ($n = 3$), and in rat lungs with varying severity of MCT-induced pulmonary hypertension ($n = 3$) compared with control animals ($n = 5$ for both rats and mice; $n = 3$ experiments per patient or per animal for each pulmonary vascular resistance [PVR] or mean pulmonary arterial pressure [PAP] listed, and significance is compared with control group). In all experiments, the level of miR-204 is relative to the control RNA U6. Data are expressed as means ± SEM (*, $P < 0.05$; **, $P < 0.01$; ***, $P < 0.001$).

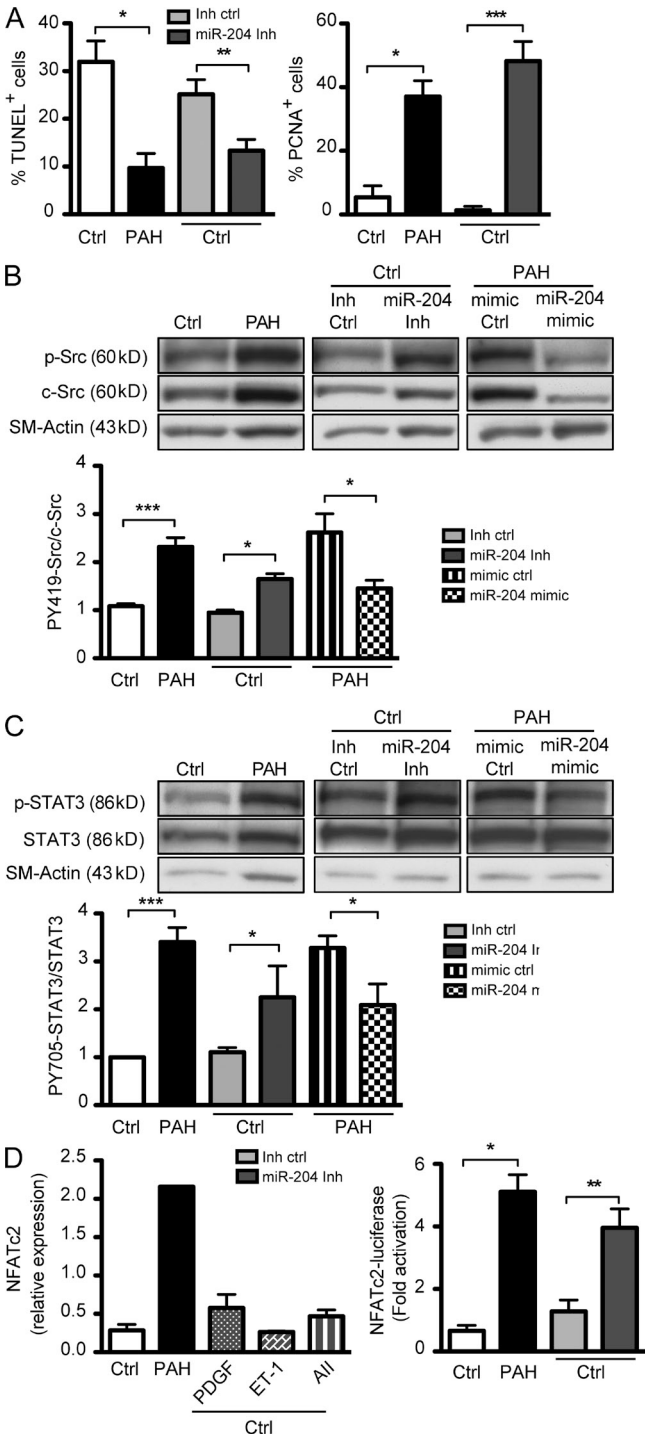

Figure 2. miR-204 modulates the Src–STAT3–NFATc2 pathway in PASMCs from a patient with PAH (PAH-PASMCs). (A) miR-204 regulates human PASMC apoptosis and proliferation. Analysis of PASMC proliferation (PCNA nuclear localization) and serum starvation–induced apoptosis (TUNEL staining) of PASMCs from PAH patients ($n = 3$ patients) and healthy controls ($n = 5$ individuals). Control (Ctrl) or miR-204 antagomirs (Inh) were added as indicated. (B and C) miR-204 down-regulation in PAH-PASMCs increases Src and STAT3 activation. Total and phosphorylated Src (B) and total and phosphorylated STAT3 (C) in PASMCs from three PAH and five control patients monitored by Western blots are shown. Control or miR-204 antagomirs or mimics were added when indicated. Smooth muscle actin (SM-actin) was used as a loading control. Representative Western blots are shown. (D) miR-204 down-regulation in PAH-PASMCs increases NFAT expression and activation in human PASMCs. NFATc2 mRNA expression (left) and activity (right) were measured by qRT-PCR (left) and luciferase assay (right) in PASMCs from control or PAH patients treated either with control or miR-204 antagomir. Error bars represent mean value ± SEM (*, $P < 0.05$; **, $P < 0.01$; ***, $P < 0.001$).

Altering miR-204 level promotes the activation of the pro-proliferative and antiapoptotic Src–STAT3–NFAT pathway in PAH-PASMCs

The increase in PASMC proliferation and resistance to apoptosis observed in PAH has been linked to the activation of the Src–STAT3–BMPR2 (Wong et al., 2005; Brock et al., 2009) and NFAT pathways (Bonnet et al., 2007b). The putative implication of miR-204 in these pathways was thus investigated. As expected, we observed an increase in the activity of Src (increased phosphorylated Src [p-Src]/Src ratio; Fig. 2 B), STAT3 (increased p-STAT3/STAT3 ratio and p-STAT3 nuclear translocation; Fig. 2 C and Fig. S3 A), and NFATc2 (increased expression, nuclear translocation, and luciferase activity; Fig. 2 D and Fig. S3 A) in PAH-PASMCs. An increase in miR-204 level altered the activation of Src, STAT3, and NFATc2 in PAH-PASMCs, whereas a decrease of miR-204 promoted them in control PASMCs (Fig. 2 and Fig. S3). These findings demonstrate that a down-regulation of miR-204 leads to the activation of the Src–STAT3–NFAT pathway in PAH-PASMCs. Activation of STAT3 was also confirmed in lung biopsies from PAH patients (Fig. S3 B), whereas NFATc2 activation in PAH lungs has been previously shown by our group (Bonnet et al., 2007b).

Next, we attempted to identify the mechanism responsible for down-regulating miR-204 in PAH-PASMCs. By stimulation experiments, we found that miR-204 expression is down-regulated by PDGF, endothelin-1, and angiotensin II, which are all well known to be involved in the pathogenesis of pulmonary hypertension (Zhao et al., 1996; Archer and Rich, 2000). Because PDGF, endothelin-1, and angiotensin II signaling is mainly mediated by STAT3 (Yellaturu and Rao, 2003; Banes-Berceli et al., 2007), the effect of STAT3 inhibition by small interfering RNA (siRNA) on miR-204 was also investigated. We observed that siSTAT3 abolished the down-regulation of miR-204 seen in PAH-PASMCs (Fig. 3 A). Finally, we found that miR-204 expression was inversely correlated with STAT3 activation, i.e., the higher STAT3 was activated, the stronger miR-204 was down-regulated (Fig. 3 B). The coding sequence of miR-204 lies within intron 6 of the human TRPM3 (transient receptor potential melastatin 3; Wang et al., 2010). A previous study revealed that miR-204 and TRPM3 share the same regulatory motif for transcription and are derived from a single transcription unit (Wang et al., 2010). This was confirmed in PAH and in control PASMCs exposed to pro-PAH factors (Fig. 3 C). To further demonstrate the implication of STAT3 in the regulation of miR-204 expression, we performed promoter region analysis of TRPM3 using ENCODE (encyclopedia of DNA elements) chromatin

immunoprecipitation (ChIP) sequencing (seq; ChIP-seq) data for the STAT family of transcription factors and identified three putative STAT-binding sites located nearby the promoter region of TRPM3 (Fig. S3 C). We therefore tested whether STAT3 can bind directly to these regulatory sites. ChIP using p-STAT3 antibody followed by PCR brought direct support for a STAT3–TRPM3 interaction (Fig. 3 D). These data suggest that STAT3 may diminish the TRPM3/miR-204 gene locus, leading to the activation of Src and NFAT.

In human vascular smooth muscle cells, the down-regulation of TRPM3 promotes IL-6 production by an undiscovered mechanism (Naylor et al., 2010). As TRPM3 is down-regulated in PAH (Fig. 3 C) and IL-6 has been reported to be increased in PAH (Humbert et al., 1995), TRPM3 might be implicated in the etiology of PAH and thus could account for the PAH phenotype. Nonetheless, TRPM3 inhibition using siRNA in control PASMCs did not mimic the PAH phenotype (no changes in $[Ca^{2+}]_i$, DYm, and PASMC proliferation and apoptosis; Fig. S4). These effects were not associated with miR-204. Indeed, as miR-204 is localized within an intronic region of TRPM3, siTRPM3 did not affect miR-204 levels (Fig. S4). Moreover, we demonstrate that miR-204 effects are not mediated by TRPM3 as within 48 h, ectopic increases of miR-204 inhibit the Src–STAT3 axis, decreasing PAH-PASMC proliferation, resistance to apoptosis, and IL-6 secretion without restoring TRPM3 expression, whereas miR-204 down-regulation in control PASMCs mimics PAH without decreasing TRPM3 (Fig. S4, A and B; Wang et al., 1999). The fact that miR-204 regulates IL-6 secretion (Fig. S4 B) and increases Src activity (Fig. 2) in PAH-PASMCs (which had been linked to several pathophysiological processes seen in PAH such as cell proliferation [Steiner et al., 2009] and migration and K^+ channel inhibition [Wong et al., 2005], as well as BMPR2 down-regulation [Wong et al., 2005]) suggests that miR-204 down-regulation might indirectly down-regulate BMPR2. We showed a significant up-regulation of BMPR2 in both human PAH-PASMCs and in PAs from PAH rats treated with miR-204 mimic (Fig. S5, A and B). This could result from the inhibition of STAT3 by the increase in miR-204, which would block the previously described STAT3-dependent BMPR2 down-regulation (Brock et al., 2009) because siSTAT3 also increases BMPR2 expression in human PAH-PASMCs (Fig. S5, A and B).

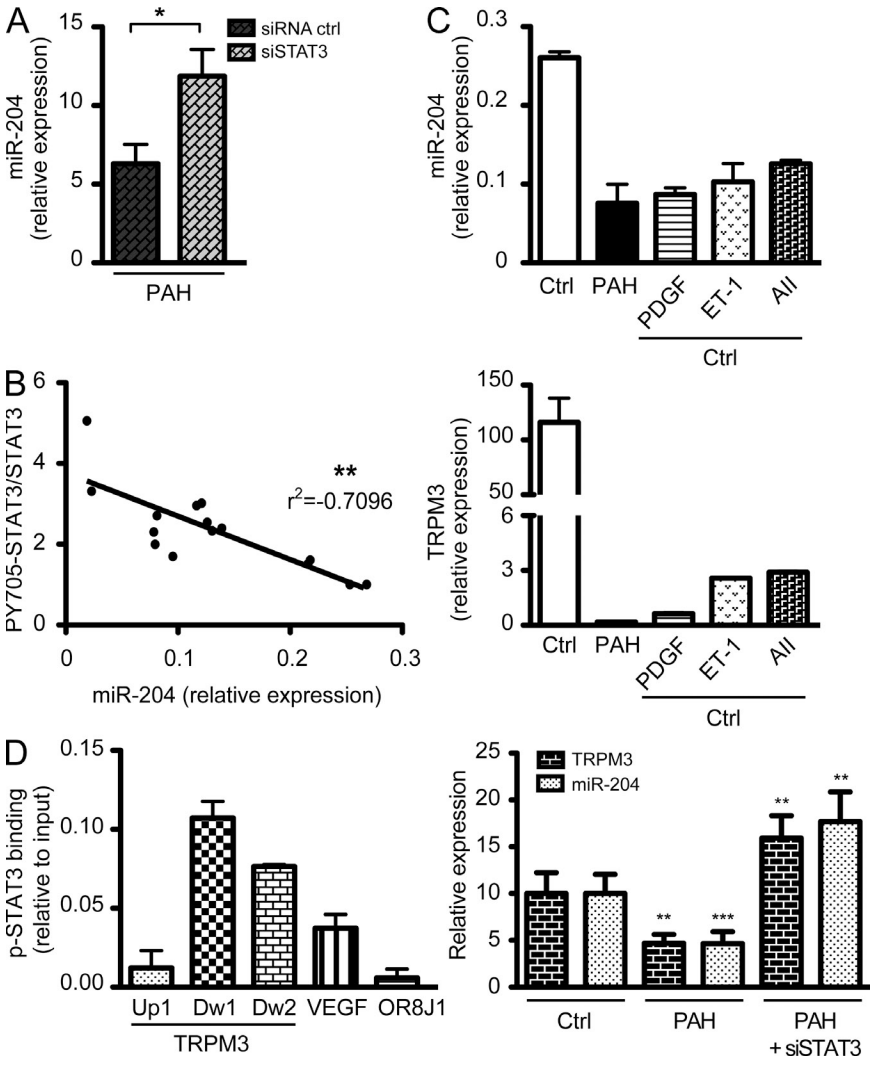

Figure 3. A primary STAT3 activation by circulating pro-PAH factors accounts for miR-204 down-regulation in PAH-PASMCs. (A) siSTAT3 increases miR-204 expression in PAH-PASMCs. miR-204 level measured by qRT-PCR in PAH treated with control siRNA (siRNA ctrl) or siSTAT3 as indicated ($n = 3$). (B) STAT3 activation and miR-204 expression are inversely correlated in PASMCs. Analysis of the correlation between STAT3 activation (measured by the pY705-STAT3/STAT3 ratio monitored by Western blot) and miR-204 expression (measured by qRT-PCR; $n = 2$ experiments/patient in three PAH and five control patients). (C) Pro-PAH factors decrease miR-204 and TRPM3 expression similarly by a STAT3-dependent mechanism in control PASMCs. miR-204 (top) and TRPM3 (middle) expression were measured by qRT-PCR performed on control cells treated with the pro-PAH factors PDGF, endothelin-1 (ET-1), or angiotensin II (AII) as indicated ($n = 3$ experiments/patient/in three PAH and five controls). (bottom) Analysis of the similarities between miR-204 and TRPM3 pattern of expression measured by qRT-PCR in control, PAH, and PAH treated with siSTAT3 as indicated. (D) p-STAT3–binding sites are detected downstream of the *TRPM3* gene. ChIP-PCR experiments studying STAT3-binding sites upstream (Up1) and downstream (Dw1 and Dw2) on *TRPM3* genes. The *OR8J1* gene was used as a negative control, whereas the *VEGF* gene was used as a positive control. Graphs represent means ± SEM (*, $P < 0.05$; **, $P < 0.01$; ***, $P < 0.001$).

Src activation by miR-204 promotes STAT3 and NFAT activation in PAH-PASMCs

From in silico analysis using TargetScan 5.1, neither STAT3 nor NFATc1, -c2, or -c3 (three NFAT isoforms activated in PAH-PASMCs; Bonnet et al., 2007b) is a predicted target of miR-204. But because a decrease in miR-204 expression increases STAT3 and NFAT activation (Fig. 2, B and C), miR-204 may be indirectly implicated in both STAT3 and NFAT activation. STAT3 activation mostly results from the activation of either the JAK2 or Src pathways (Gharavi et al., 2007; Cheranov et al., 2008; Li et al., 2008). Interestingly, among all the predicted targets of miR-204, JAK2 as well as two Src activators (SHP2 [Wu et al., 2006] and SHC [Src homology 2 domain containing; Sato et al., 2002]) were identified. Among JAK2, SHP2, and SHC, only SHP2 was up-regulated in PAH-PASMCs (Fig. 4 A and Fig. S5 C). Moreover, increasing miR-204 level in PAH-PASMCs decreased SHP2, whereas miR-204 inhibition in control PASMCs cells increased SHP2 expression (Fig. 4 A). These results suggest that SHP2 may be the primary target of miR-204 in PAH. To test this hypothesis, we performed a reporter assay in which the luciferase reporter gene was under control of the SHP2 3′ UTR. We observed that both point mutations that abrogate the binding site of miR-204 in SHP2 3′ UTR as well as the sequestration of miR-204 with a specific inhibitor increase the expression of the luciferase reporter, confirming the implication of miR-204 in the regulation of SHP2 mediated through its 3′ UTR (Fig. 4 B). Finally, as expected, the SHP2-dependent activation of Src

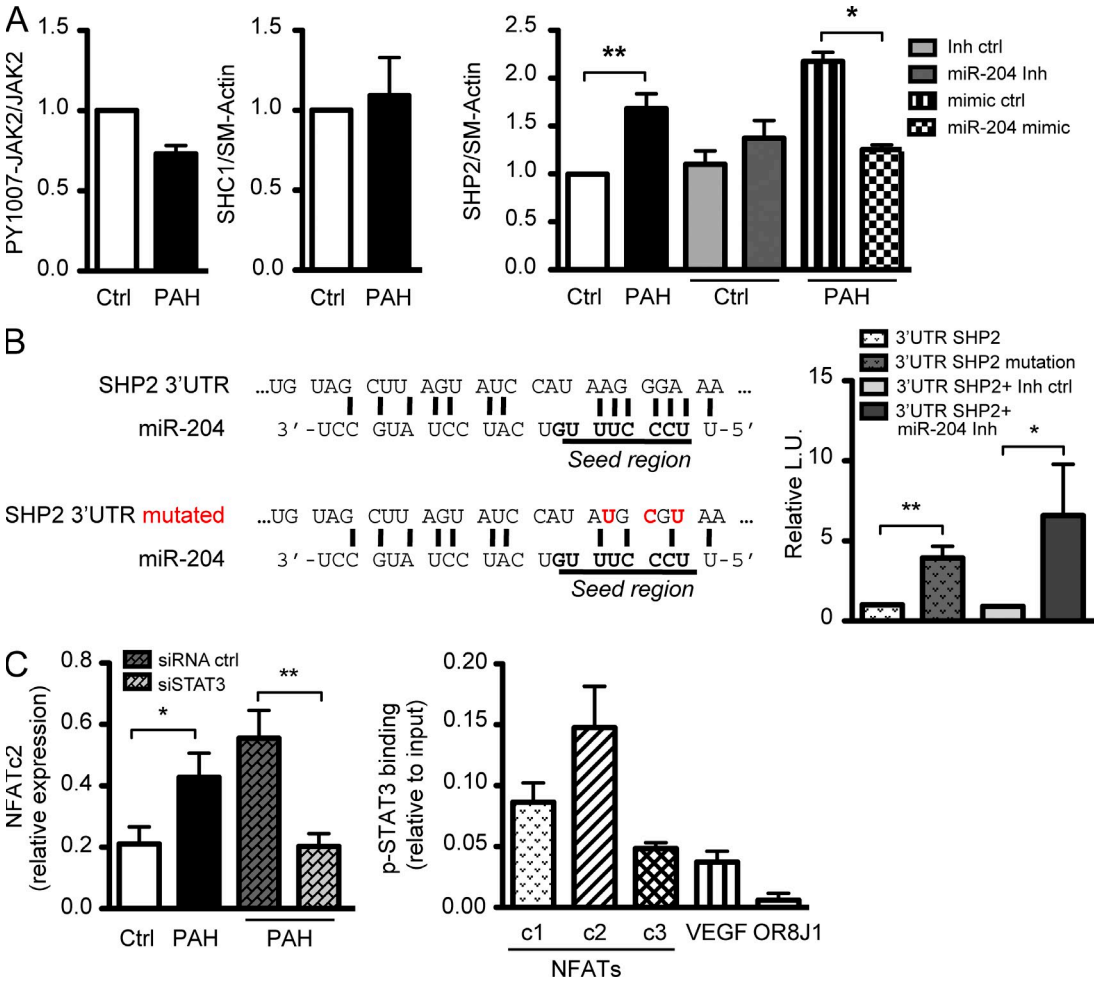

Figure 4. SHP2 up-regulation by miR-204 promotes activation of the Src–STAT3–NFAT axis in PAH-PASMCs. (A) SHP2 is up-regulated by miR-204 in PAH-PASMCs. Total and phosphorylated JAK2 (left), SHC1 (middle), and SHP2 (right) protein expression was monitored by Western blot ($n = 3$ independent experiments) in PASMCs from three PAH and five control patients. (right) miR-204 antagomir (Inh) and mimic along with appropriate controls (Ctrl) were added as indicated. SM-actin, smooth muscle actin. (B) miR-204 directly targets the SHP2 3′ UTR. (left) Binding sites of miR-204 found in the 3′ UTR of SHP2. Mutations introduced into the luciferase reporter are shown in red. (right) Relative firefly luciferase activity derived from the SHP2 3′ UTR and SHP2 3′ UTR mutated reporter constructs monitored after transfection in control PASMCs ($n = 5$). Control and miR-204 inhibitor ($n = 3$) were added as indicated. L.U., luciferase unit. (C) STAT3 regulates NFATc2 expression. NFATc2 mRNA level (left) relative to 18S measured by qRT-PCR in PASMCs from control and PAH patients treated when indicated with control or STAT3 siRNA ($n = 3$ qRT-PCR/patient in three PAH and five control patients). ChIP-PCR experiments (right) studying STAT3 binding on genes encoding the indicated *NFAT* isoforms (NFATc1, -c2, and -c3). The *OR8J1* gene was used as a negative control, whereas the *VEGF* gene was used as a positive control. Graphs represent means ± SEM (*, $P < 0.05$; **, $P < 0.01$).

accounts for an increase in STAT3 activation in PAH-PASMCs as either SHP2 knockdown by siRNA or the Src inhibitor PP2 (4-amino-5-(4-chlorophenyl)-7-(*t*-butyl)pyrazolo[3,4-*d*]pyrimidine) significantly decreases STAT3 activation in PAH-PASMCs (Fig. S6 A). Thus, the attenuation of miR-204 level promotes SHP2 expression, thereby leading to Src activation and thus enhancing STAT3 activation.

NFAT activation mainly results from the activation of either calcineurin (Macian, 2005) or Pim-1 (Glazova et al., 2005), but none of them are predicted targets of miR-204. This was confirmed by luciferase assay (Fig. S6 B). The ChIP-seq data revealed the presence of several STAT-binding sites surrounding NFAT genes (Fig. S6 C; Chen et al., 2008; Bourillot et al., 2009). Thus, we inferred that SHP2–Src activation results in STAT3 activation, which in turn activates NFAT in PAH-PASMCs. To demonstrate the implication of STAT3 in the regulation of NFATc2 expression in PAH, the effect of STAT3 knockdown on NFATc2 expression was measured in PAH-PASMCs and control PASMCs. When compared with PAH-PASMCs treated with control siRNA, PAH-PASMCs exposed to siRNA targeting STAT3 exhibited significantly reduced NFATc2 expression (Fig. 4 C), suggesting that STAT3 activation leads to NFATc2 expression in PAH-PASMCs. Moreover, ChIP analyzed by real-time PCR (ChIP-PCR) confirmed the binding of STAT3 on the *NFATc2* gene (Fig. 4 C). NFAT activation by SHP2–Src has been described in skeletal muscle (Fornaro et al., 2006), and our findings not only confirm this previous finding but provide an additional mechanism implying STAT3.

Increasing miR-204 level in PAH-PASMCs reverses the pro-proliferation and antiapoptotic phenotype of PAH-PASMCs

In PAH-PASMCs, Src–STAT3–NFAT-mediated proliferation (Wong et al., 2005; Bonnet et al., 2007b) has been linked to the down-regulation of K^+ channels (Platoshyn et al., 2000; Bonnet and Archer, 2007), resulting in membrane depolarization (Yuan, 1995; Platoshyn et al., 2000), opening the voltage-dependent Ca channels, thereby increasing intracellular Ca concentration ($[Ca^{2+}]_i$; Yuan, 1995; Wong et al., 2005; Bonnet et al., 2007b). Using Fluo-3AM and proliferating cell nuclear antigen (PCNA), we measured the effect of miR-204 modulation on $[Ca^{2+}]_i$ and PASMC proliferation. The miR-204 inhibition in control PASMCs increases $[Ca^{2+}]_i$ and PASMC proliferation to the level seen in PAH-PASMCs, whereas the increase of miR-204 level in PAH-PASMCs decreases $[Ca^{2+}]_i$ and proliferation to a level similar to that seen in control PASMCs (Fig. 5, A and C). To further confirm that these effects were mediated via the Src–STAT3 and NFAT pathway, we treated cells with the Src inhibitor PP2, STAT3 siRNA, and the NFAT inhibitor VIVIT (Bonnet et al., 2007b). As expected, VIVIT treatment does not further decrease $[Ca^{2+}]_i$ in PAH-PASMCs in which the miR-204 level has been re-established (Fig. 5, A and C), whereas in PAH-PASMCs, PP2 and siSTAT3 decrease $[Ca^{2+}]_i$ to a level similar to that seen in control PASMCs (Fig. 5 B). Similarly to SHP2 inhibition (siSHP2), the decrease in $[Ca^{2+}]_i$ resulting from increasing the miR-204 level in PAH-PASMCs inhibits cell proliferation (PCNA; Fig. 5 C). In addition to the STAT3–NFAT axis, the antiproliferative and proapoptotic effect of SHP2 inhibition by siRNA or miR-204 mimic could also be attributed to the inhibition of the RhoA–ROCK (Rho-associated, coiled-coil–containing protein kinase) pathway (Fig. S6 D; Lee and Chang, 2008; Kimura and Eguchi, 2009), which is increased and implicated in PAH-PASMC proliferation (Barman et al., 2009).

Based on the fact that miR-204 is encoded within TRPM3 (Wang et al., 2010) and TRPM3 expression modulation may account for changes in $[Ca^{2+}]_i$, we tested whether miR-204–dependent modulation of $[Ca^{2+}]_i$ could be attributed to TRPM3. We demonstrated that restoring miR-204 constitutes the primary therapeutic target, as TRPM3 inhibition by siRNA (which did not affect miR-204 expression as miR-204 is located within an intronic region) did not affect $[Ca^{2+}]_i$ and PASMC proliferation (Fig. S4).

Resistance to apoptosis observed in PAH-PASMCs has been linked to mitochondrial membrane potential ($\Delta\Psi_m$) hyperpolarization, which would block the release of proapoptotic mediators like cytochrome *c* (Bonnet et al., 2007a, b, 2009). Using tetramethylrhodamine methyl ester (TMRM), we measured whether miR-204 modulation can affect mitochondrial hyperpolarization. We observed that miR-204 inhibition in control PASMCs hyperpolarizes $\Delta\Psi_m$ to a level similar to that observed in PAH-PASMCs (Fig. 5 D), whereas either increasing the miR-204 level or using SHP2 siRNA, Src inhibitor PP2, or STAT3 siRNA in PAH-PASMCs depolarizes $\Delta\Psi_m$ to a level similar to that measured in control PASMCs (Fig. 5 E). Finally, mitochondrial depolarization induced by up-regulating miR-204 expression in PAH-PASMCs increases serum starvation–induced apoptosis (terminal deoxynucleotidyl transferase dUTP nick end labeling [TUNEL]; Fig. 5 F). As for $[Ca^{2+}]_i$, $\Delta\Psi_m$ was not affected by TRPM3 inhibition (Fig. S4).

The STAT3–miR-204–Src–STAT3–NFAT axis is activated in the PAH animal model

We next tested the contribution of miR-204 in the MCT-injected rat model of PAH (Frasch et al., 1999; Bonnet et al., 2007b). We observed that miR-204 down-regulation parallels PAH development, confirming that the decreasing of miR-204 level correlates with PAH progression and severity (Fig. 6, A and E). To further study the timing of activation of the STAT3–miR-204–Src–STAT3–NFAT axis in the progression of PAH, rats were sacrificed at various intervals after the injection of MCT. Before sacrifice, pulmonary arterial pressure was measured directly by right heart catheterization in closed chest rats. We observed an increase in STAT3 activation (≤1 wk; Fig. 6 C) preceding miR-204 down-regulation (occurring 2 wk after MCT injection). Once miR-204 is down-regulated (≥2 wk), SHP2 is increased and STAT3 activation is pushed up to reach and sustain a maximal level from week 2–4 (Fig. 6, B and C). Once STAT3 activation becomes maximal, NFAT gets activated (≥3 wk; Fig. 6 D), increasing pulmonary arterial pressure (Fig. 6 E). Therefore, the

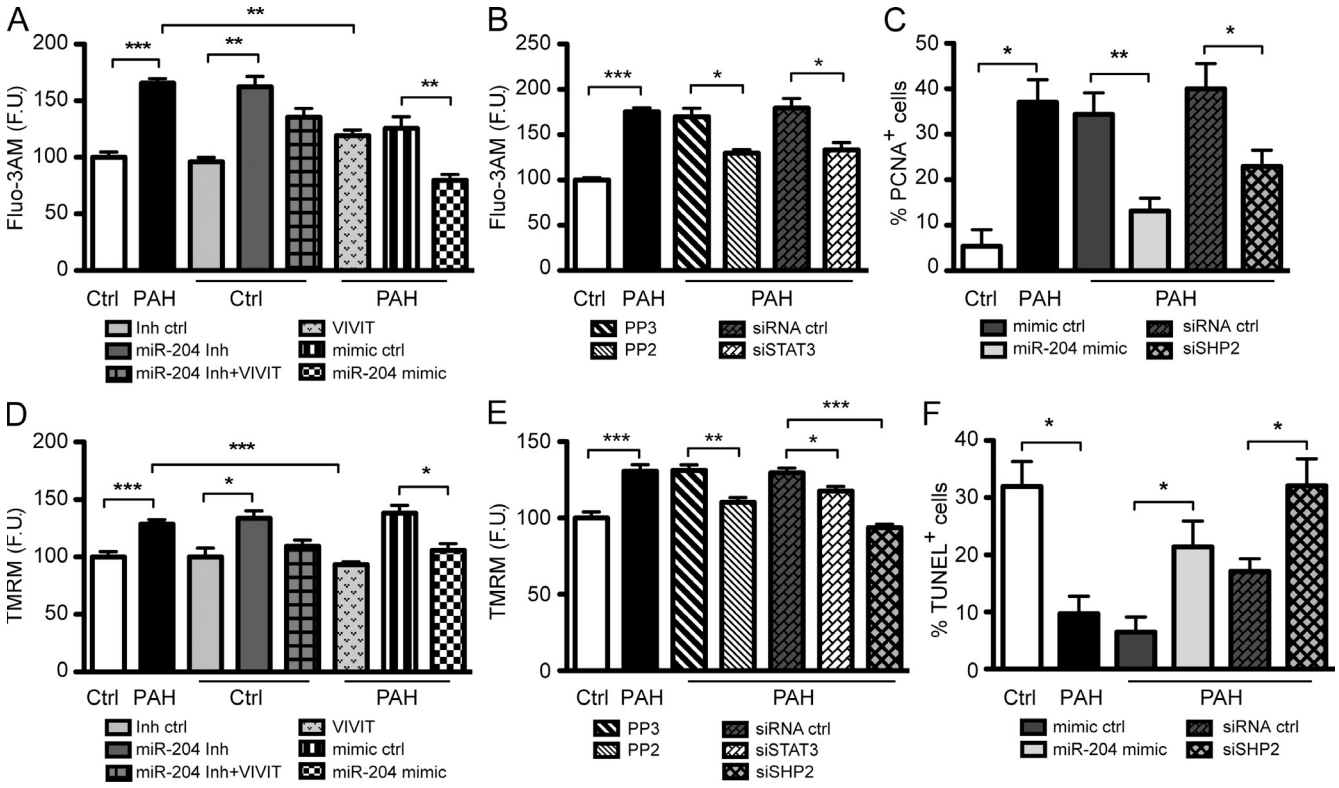

Figure 5. miR-204 restoration decreases $[Ca^{2+}]_i$ and depolarizes mitochondrial membrane potential. (A–C) Analysis of $[Ca^{2+}]_i$ (Fluo3-AM) and cell proliferation (PCNA nuclear localization) of PASMCs from PAH and control (Ctrl) patients. miR-204 antagomir (Inh) and mimics, VIVIT (NFAT competitor peptide), and PP2 (Src inhibitor) compared with PP3, its negative control, STAT3 siRNA, SHP2 siRNA, and appropriate controls for each treatment were added as indicated (n = 50–150 cells/patient in three PAH and five control patients). (D–F) Analysis of the mitochondrial membrane potential ($\Delta\Psi_m$; TMRM) and serum starvation–induced apoptosis (TUNEL staining) of PASMCs from PAH and control patients. miR-204 antagomir (Inh) and mimics, VIVIT (NFAT competitor peptide), PP2 (Src inhibitor), STAT3 siRNA, SHP2 siRNA, and appropriate controls for each treatment were added as indicated (n = 50–150 cells/patient in three PAH and five control patients). F.U., fluorescence unit. Graphs represent means ± SEM (*, P < 0.05; **, P < 0.01; ***, P < 0.001).

time course analysis confirms our in vitro data supporting the idea that the activation of STAT3 occurs before the decrease in miR-204, which thereby amplifies the activation of STAT3 and NFAT. These results confirmed the initial implication of STAT3 in the attenuation of miR-204 in PAH. Once miR-204 is down-regulated, STAT3 activation is further increased and maintained over a long period of time, thus allowing NFAT-dependent PASMC proliferation and resistance to apoptosis and increasing PA remodeling and pressures.

Nebulization of miR-204 mimics reverses MCT-induced PAH

To test whether restoration of miR-204 level can reverse symptoms of PAH in the rat model, synthetic miR-204 RNA molecules were selectively delivered to the lung of

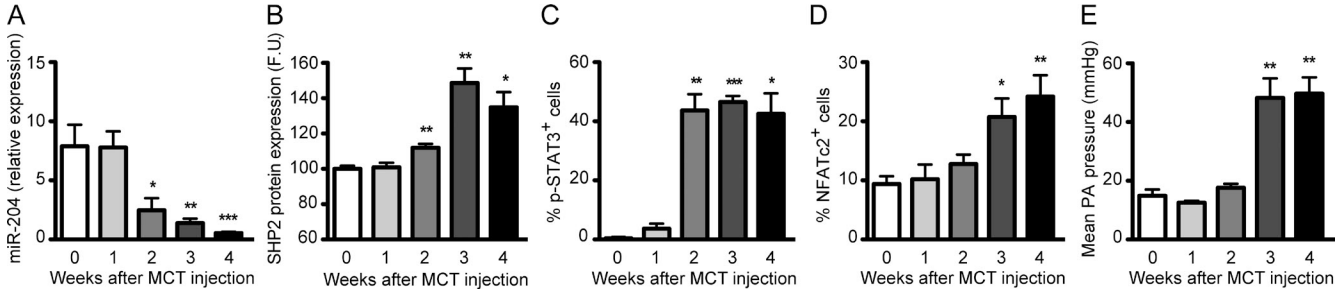

Figure 6. miR-204 level decreases within distal PAs of rats injected with MCT during the fourth week of PAH development. (A) miR-204 expression relative to U6 measured by qRT-PCR in distal PAs of rats. (B) SHP2 protein expression was quantified in distal PAs by immunofluorescence (F.U., fluorescent unit) on lung sections (n = 5 measurements by rat in five rats per time point). (C and D) STAT3 and NFAT activation were measured by the percentage of cells presenting p-STAT3 and NFAT nuclear localization, respectively, in distal PAs of rats (n = 5 measurements by rat in 10 rats per time point). (E) Mean PA pressure measured by right catheterization in closed chest rats (n = 5 rats per group). Graphs represent means ± SEM (*, P < 0.05; **, P < 0.01; ***, P < 0.001).

MCT-induced PAH (MCT-PAH) rats 10–15 d after MCT injection (when endogenous miR-204 down-regulation reached its peak and PAH was established) by intratracheal nebulization. To verify the tissue distribution of nebulized miR-204, we measured miR-204 mRNA levels in several tissues by qRT-PCR, and we analyzed by immunofluorescence the distribution of the mimic DY547 labeled (control of transfection; Fig. S7 A). Our results revealed that nebulized synthetic miR-204 is essentially localized to intraparenchymal resistance PAs and therefore has limited, if any, detrimental effect.

A longitudinal study to assess the efficacy of our treatment was performed for 2 wk using noninvasive measurements (Doppler echocardiography). We observed that the local delivery of synthetic miR-204 in MCT-PAH rats reduced pulmonary arterial pressure (Fig. 7 A), as assessed by the PA acceleration time (PAAT), a Doppler parameter linked to PA pressure (PAAT being inversely correlated to PA pressure; Fig. S7 B). In addition, synthetic miR-204 decreased right ventricle wall thickness (Fig. S7 B) when compared with MCT-PAH rats treated with nonspecific synthetic RNA molecules. In an opposite manner, miR-204 antagomir nebulization in control rats induced PAH development within 3 wk (Fig. 7 A and Fig. S7 B), whereas antagomir negative control nebulized to two animals had no effects (not depicted). To determine whether synthetic miR-204 delivery can reduce PA remodeling in MCT-PAH animals, we measured medial wall thickness. We observed that animals treated with the synthetic miR-204 displayed a significant reduction in medial thickness of small (≤300 µm) and medium-sized (≤600 µm) PAs (Fig. 7 B). A significant decrease of SHP2, p-STAT3, NFATc2 activation, PASMC proliferation (as assessed by PCNA distribution), and resistance to apoptosis (TUNEL) was also observed in rats treated with synthetic miR-204 (Fig. 7 C and Fig. S8).

DISCUSSION

Although a previous study has reported that several miRNAs were aberrantly expressed in PAH (Caruso et al., 2010), our study is the first providing a mechanistic approach to their

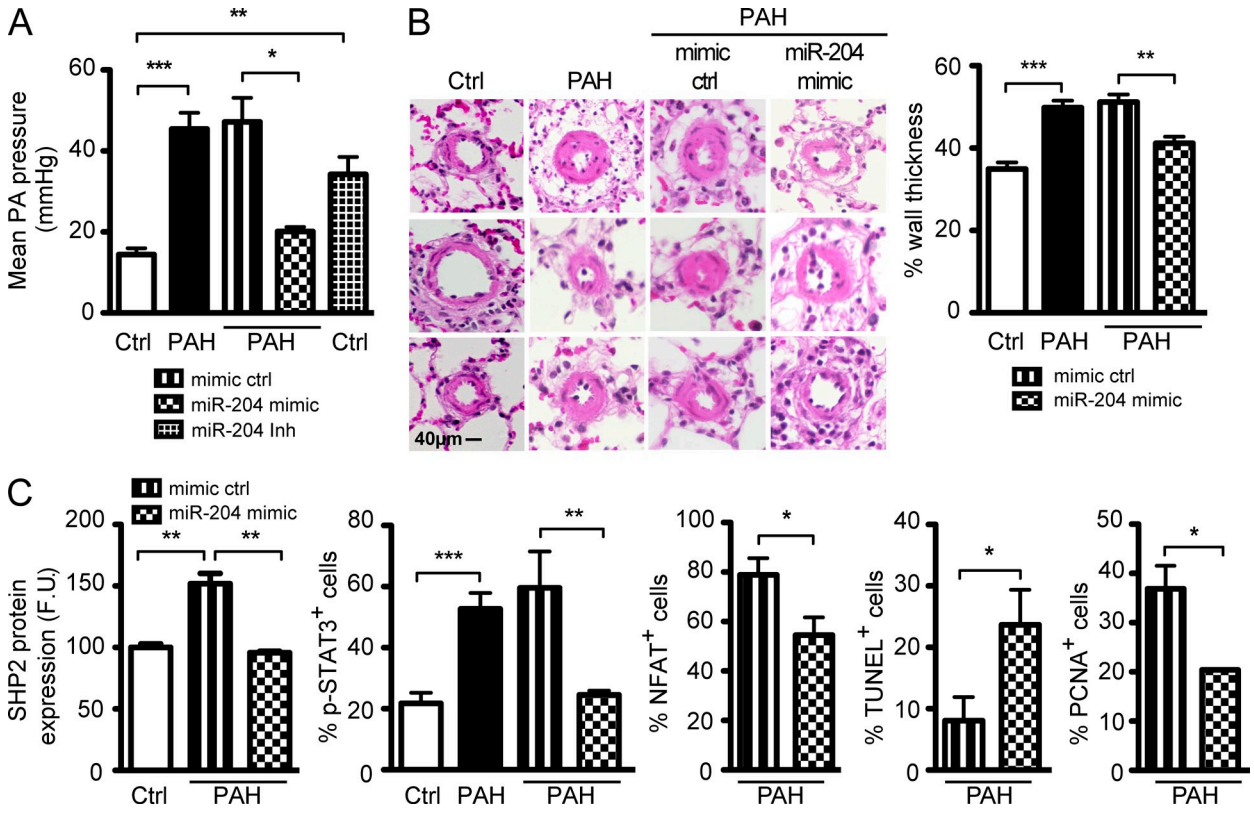

Figure 7. Increasing the level of miR-204 by nebulization reverses MCT-PAH. (A) miR-204 restoration decreases mean PA pressure. Mean PA pressure measured by right catheterization in closed chest rats (n = 5 rats per group) is shown. miR-204 antagomir (Inh) and mimic along with appropriate controls (Ctrl) as indicated were intratracheally nebulized after 2 wk of MCT injection. (B) miR-204 restoration decreases PA wall thickness. PA remodeling was measured by the percentage of media wall thickness on lung sections stained by hematoxylin and eosin (n = 5 measurements/rat in 10 rats). The pictures shown illustrate representative distal arteries, and the graph represents mean values. (C) By decreasing SHP2, STAT3, and NFAT activation, miR-204 restoration increases apoptosis and decreases proliferation in MCT-rat PASMCs. SHP2 protein expression (left) was quantified in distal PAs by immunofluorescence (F.U., fluorescent unit) on lung sections; STAT3 and NFAT activation (middle) measured by the percentage of cells presenting p-STAT3 and NFAT nuclear localization, respectively, in distal PAs of rats; apoptosis and proliferation measured by the percentage of cells presenting TUNEL and PCNA nuclear localization, respectively, in distal PAs of rats. Control and miR-204 mimic were intratracheally nebulized after 2 wk of MCT injection as indicated (n = 5 measurements by rat in five rats per group). Graphs represent means ± SEM (*, P < 0.05; **, P < 0.01; ***, P < 0.001).

implication in the etiology of human PAH. Despite the fact that several other miRNAs are aberrantly expressed in PAH-PASMCs, we focused our study on miR-204, which was the only one down-regulated, and because putative mRNA targets predicted in silico (TargetScan 5.1) were members of pathways implicated in cell proliferation and resistance to apoptosis, including Src (Wong et al., 2005), STAT3 (Shibata et al., 2003), and NFAT (Fig. S1; Bonnet et al., 2009). Because miR-204 is expressed seven times more in PASMCs than PAECs, we focused our research on the role of miR-204 in PAH-PASMC proliferation and resistance to apoptosis, although we cannot exclude a role of miR-204 in PAH-PAECs, which are also implicated in PAH etiology (Jurasz et al., 2010).

Other miRNAs have been implicated in vascular diseases, but their implication remains elusive. For example, although a recent study has shown that miR-21 up-regulation was implicated in vascular neointimal lesions (Ji et al., 2007), miR-21 has been shown to be down-regulated in lung tissue of MCT rats and unchanged in chronic hypoxia (Caruso et al., 2010). Interestingly, in our human PAH-PASMCs, miR-21 is unchanged, suggesting that miR-21 might not necessarily be an important player in the etiology of PAH. Interestingly, in the Caruso et al. (2010) study, miR-204 is down-regulated by 45% and 40% in both chronic hypoxic and MCT rat lungs, respectively, confirming our findings in PASMCs and human lungs.

The role of miR-204 in vascular tissues remained unknown. A recent study performed in retinal epithelial cells and several cancer cells has demonstrated that the down-regulation of miR-204 is associated with enhanced PDGFb expression, cell proliferation, and the down-regulation of K^+ channels, which in turn depolarizes epithelial cell membrane potential (Wang et al., 2010). These findings are consistent with ours and with the already known pathophysiological processes of PAH, reinforcing the importance of miR-204 in the etiology of PAH. Indeed, increased PDGFb has been reported in PAH (Barst, 2005), and this is consistent with STAT3 activation (PDGFb being an activator of STAT3; Yu et al., 2003), PASMC proliferation, and resistance to apoptosis (Bonnet et al., 2009).

miR-204 is encoded within the *TRPM3* gene. Although, transient receptor potential cation channels have been implicated in PAH (Yu et al., 2004), the role of TRPM3 remains unknown. In our study, we demonstrate that miR-204 effects are not mediated by TRPM3. First, ectopic increases of miR-204 inhibit the SHP2–Src–STAT3 axis, decreasing PAH-PASMC proliferation, resistance to apoptosis, and IL-6 secretion without restoring TRPM3 expression (Fig. S4, A and B). Second, miR-204 down-regulation in control PASMCs mimics PAH, without decreasing TRPM3 (Fig. S4 A). Third, TRPM3 inhibition (without affecting miR-204 levels) did not induce a PAH phenotype in control PASMCs (Fig. S4 C).

Recently, a study performed in human PASMCs linked the down-regulation of BMPR2 to the activation of an IL-6–STAT3–miR-17-92 axis (Brock et al., 2009). In their model, IL-6 activates STAT3, thereby increasing the miR-17-92 cluster expression and down-regulating BMPR2. Despite the fact that miR-17-92 cluster expression is unchanged in our PAH-PASMCs, our study offers a new perspective on the mechanism of BMPR2 down-regulation in PAH. The fact that miR-204 regulates IL-6 secretion (Fig. S4 B) and increases Src activity (Fig. 2) in PAH-PASMCs suggests that miR-204 down-regulation might indirectly down-regulate BMPR2. This is supported by preliminary data showing a significant up-regulation of BMPR2 in both human PAH-PASMCs and in PAs from PAH rats treated with miR-204 mimic (Fig. S5).

One major strength of the present study is the clear demonstration of a mechanism for the origin of the miRNA deregulation in ∼10 PAH patients that we provide for the first time in the field of vascular diseases. We show that a primary STAT3 activation by circulating pro-PAH factors such as endothelin-1, PDGF, and angiotensin II (which all increase at the onset of PAH; Archer and Rich, 2000) accounts for the down-regulation of miR-204 in control PASMCs. This finding was confirmed by both promoter analysis and ChIP-PCR analysis, which show a direct binding of STAT3 near the *miR-204* gene (within *TRPM3*; Fig. 3 D). Moreover, we showed that the activation of STAT3 in vivo in PAs of rats injected with MCT precedes miR-204 down-regulation (Fig. 6 C). Once miR-204 is down-regulated, the Src activator SHP2 is directly up-regulated and IL-6 (Fig. S4 B) and PDGF production (Wang et al., 2010) increased, reinforcing STAT3 activation via Src and allowing NFAT activation. This could explain the sustained pro-proliferative and antiapoptotic phenotype of cultured PAH-PASMCs. The activation of such a mechanism is in accordance with a recently published RNA profiling study performed in 18 iPAH patients (Rajkumar et al., 2010). A reanalysis of the data available for this study confirms the down-regulation of TRPM3 as well as the up-regulation of both SHP2 (also known as PTPN11) and NFATc2. Although we provide evidence that STAT3 increases NFAT expression by binding to the *NFAT* genes promoter region, the activation of NFAT by STAT3 requires the activation of either the Ca–calcineurin pathway or the activation of other NFAT activators like Pim-1. In our model, $[Ca^{2+}]_i$ is indeed increased, which could participate in calcineurin activation. Moreover, Pim-1 is a protooncogene that is regulated by STAT3 and that increases in vascular diseases (Katakami et al., 2004). It is therefore possible that STAT3 activation not only accounts for NFAT expression but also promotes NFAT activation by up-regulating Pim-1 expression (Rainio et al., 2002). Finally, we measured miR-204 expression in buffy coats of 13 PAH patients and 7 control donors and showed that as in PAH lungs, miR-204 is down-regulated, suggesting that miR-204 could be a good PAH biomarker.

In conclusion, we herein provide the first evidence that aberrantly expressed miRNAs play a critical role in the etiology of human PAH. We demonstrate both in vitro and in vivo that miR-204 can be therapeutically targeted, leading to a decrease of proliferation, vascular remodeling, and PA blood pressure and thus represents a new therapeutic approach for

PAH. Moreover, we have preliminary evidence that miR-204 might regulate the RhoA–ROCK pathway in PAH-PASMCs (another important component of PAH; Fig. S6 D; Doggrell, 2005). Although other experiments are required to identify the exact mechanism, Bregeon et al. [2009] and Kimura and Eguchi [2009] have previously demonstrated a role of SHP2 in the RhoA–ROCK pathway. This constitutes the basis for a further investigation. Our study proposes that the therapeutic modulation of a single miRNA (miR-204) may affect many pathways simultaneously associated with PAH to achieve clinical benefit. Compared with currently used therapies that target a single protein (ET-1 receptor blockers, PDE5 inhibitor, etc.), the regulation of hundreds of targets in multiple pathways by miRNAs may reduce the emergence of drug resistant as currently seen in PAH because many simultaneous mutations would be required to subvert the effects of miRNA expression. However, at the same time, miRNA-based therapies will require thorough preclinical validation as these broad effects may, in some cases, have toxic consequences. Nonetheless, this was not observed in our rats.

In summary, we provide a comprehensive model (Fig. S8 E) linking miRNA abnormal expression to already known pathophysiological processes in PAH, including NFAT activation, BMPR2 down-regulation, IL-6 production, the Rho pathway, PASMC proliferation, and resistance to apoptosis (Cowan et al., 2000; Sakao et al., 2005; Bonnet and Archer, 2007; Bonnet et al., 2007b; Tuder et al., 2007). Thus, our study does not only demonstrate the importance of miRNAs in PAH but also suggests that reestablishing the miR-204 level might represent a novel therapeutic approach for human PAH.

MATERIALS AND METHODS

Ethics. All experiments were performed in accordance with the Université Laval's Ethics and Biosafety Committee (protocol number 20142) and the Centre Hospitalier Universitaire de Québec's Ethics Committee. The investigation conforms to the Guide for the Care and Use of Laboratory Animals, published by the National Institutes of Health (publication no. 85–23, revised 1996) and with the principles outlined in the Declaration of Helsinki.

Human tissue samples. See Table S1. All patients gave informed consent before the study. Normal lung tissues (controls) were obtained during lung resection for benign ($n = 3$) or malignant ($n = 5$) tumors. Only the healthy parts of the lungs were used in this study. All the PAH tissues were from open lung explants from transplant or autopsy.

Cell culture. We used cells in the first to third passage. PAH-PASMCs were obtained as described previously (McMurtry et al., 2005) from ∼1,500-µm-diameter small PAs from two males with iPAH (31- and 48-yr-old patients A and B) and one female with PAH group 1 (lupus; 54-yr-old patient C) from lung explants. All patients had right catheterization that confirmed pulmonary hypertension (mean pulmonary arterial pressure >25 mmHg). Age- and sex-matched control PASMCs (three males A, B, and C 45, 21, and 64 yr old; and two females D and E 17 and 35 yr old), and PAECs were purchased from Cell Application USA. PASMCs were grown in high-glucose DME supplemented with 10% FBS (Invitrogen) and 1% antibiotic/antimitotic (Invitrogen; Bonnet et al., 2007a). STAT3 and SHP2 were inhibited by a specific siRNA (20 nM for 48 h; Applied Biosystems) as previously described (Bonnet et al., 2007a). NFAT was inhibited by 4 µM VIVIT as previously described (Bonnet et al., 2007b). Control PASMCs were exposed to 30 ng/ml PDGF, 10 nM endothelin-1, 200 nM angiotensin II, or 100 ng/ml TNF (all from EMB Canada). The Src inhibitor PP2 effects were compared with its negative control inhibitor PP3 (4-amino-7-phenylpyrazol [3,4-*d*] pyrimidine; 10 µM for 48 h). The Ca phosphate transfection method was used to transfect miRIDAN miR-204 mimics (200 nM for 48 h) or miR-204 antagomir (hairpin inhibitor at 200 nM for 48 h). For each experiment, we used a proper control (mimics or hairpin inhibitor negative control #1 from Thermo Fisher Scientific). Dose response, transfection efficiency, and siRNA efficiencies are presented in Fig. S8 C.

TaqMan low density arrays (TLDAs). TLDA was performed in four patients, two for each condition, and according to the manufacturer's protocol (Applied Biosystems). Each sample was analyzed in duplicate. Raw CTs were then normalized using two different normalization procedures, one normalizing relative to U6 small nuclear RNA and the other one relative to the median CT. An empirical Bayesian method within the package limma in Bioconductor was used to identify the significantly modulated miRNAs. miRNAs were required to be significantly modulated for both normalizations. TLDA data have been deposited in GEO DataSets under accession no. GSE21284.

DNA microarrays. DNA microarray experiments were performed using the Whole Human Genome microarray kit (Agilent Technologies). The arrays were scanned using a dual-laser DNA microarray scanner (Agilent Technologies), and the data were extracted from images using the Feature Extraction software. For the control versus PAH patient comparison, RNAs extracted from two control patients were hybridized on Cy3, and RNAs extracted from two PAH patients were hybridized on Cy5. For the miR-204 inhibition experiment, RNAs extracted from control PASMCs treated for 48 h with 200 nM miR-204 antagomir (Thermo Fisher Scientific) were hybridized with Cy3, whereas PASMCs treated with antagomir negative were hybridized on Cy5. Data were background subtracted and normalized within the array using the LOESS normalization before significant modulation assessment using the Empirical Bayes method within limma in Bioconductor. Genes listed as targets of miR-204 in TargetScan 5.1 and having a level of expression ≥100 in $\log_2$ base and being up-regulated after miR-204 inhibition were considered as miR-204 targets in our model. Microarray data have been deposited in GEO DataSets and are available under accession no. GSE21284.

qRT-PCR. To measure miR-204 expression, the mirVana kit (Applied Biosystems) was used to extract total RNA from PAH-PASMCs or control PASMCs. Stem-loop qRT-PCR for mature miRNAs was performed on a real-time PCR system (AB 7900; Applied Biosystems). Regular qRT-PCR was performed as previously described (Bonnet et al., 2007b).

ChIP-PCR. In brief, control PASMC asynchronously growing cells were treated with endothelin at 10 nM. Cross-links were generated with 1% formaldehyde, and chromatin was extracted in lysis buffer (50 mM Tris-HCl, pH 8, 10 mM EDTA, 0.2% SDS, and 5 mM Na-butyrate). Chromatin was then sheared by sonication (Bioruptor; Diagenode) on ice to a mean length of 750 bp. After preclearing with a mix of protein A/G–Sepharose beads (4°C for 1 h), 80 µg chromatin was used for immunoprecipitation with appropriate antibodies (10 ml p-Sat3 [Tyr705; 9131; Cell Signaling Technology] and 10 mg normal rabbit IgG [I-1000; Vector Laboratories]) in a total volume of 300 ml. After overnight incubation at 4°C, 25 µl of protein A Dynabeads (Invitrogen) was added and incubated for >1 h. Beads were extensively washed, and immunoprecipitated complexes were eluted in buffer E (50 mM Na bicarbonate and 1% SDS). Cross-links were reversed overnight at 65°C. Samples were treated with proteinase K, and the DNA was extracted using phenol-chloroform. Quantitative real-time PCR was performed using SYBR green I (LightCycler 480; Roche). Enrichment for a specific DNA sequence was calculated using the comparative Ct method. The numbers presented with standard errors are based on two biological repeats (cells/chromatin/immunoprecipitation). Primers used in the PCR reactions (Table S2) were analyzed for specificity, linearity range, and efficiency to accurately

evaluate occupancy (percentage of immunoprecipitation/input). Vascular endothelial growth factor (VEGF) primers were used as positive control, whereas OR8J1 primers were used as negative control.

Confocal microscopy. NFATc1 and -c2 and STAT3 nuclear translocation assays were performed using antibodies (1:250; Abcam) as previously described (Bonnet et al., 2007b). TMRM, TUNEL, PCNA, and Fluo-3 were measured as previously described (Bonnet et al., 2009; Bonnet et al., 2007b).

Transfection and luciferase assay for different 3′ UTR constructions. The 3′ UTRs of each gene of interest were cloned and inserted in the psiCHECK2 plasmid immediately downstream from the stop codon of firefly luciferase. Once ready, cells were transfected with the reporter plasmid with 200 nM of unrelated small RNA duplex (mimic control; Invitrogen), miR-204 mimic (Thermo Fisher Scientific), miR-204 inhibitor (Thermo Fisher Scientific), or with *Caenorhabditis elegans* miR-67 inhibitor used as control (Thermo Fisher Scientific). Firefly and Renilla luciferase activities were measured consecutively using a dual-luciferase assay 48 h after transfection. The presence of an interaction between miR-204 and target mRNA would reduce the firefly luciferase activity (normalized to Renilla luciferase activity expressed from the psiCHECK2 plasmid). To abrogate miR-204 binding to the SHP2 3′ UTR, point mutations were made into the 3′ UTR sequence that corresponds to the miR-204 binding site in position 2, 4, and 6 from the 5′ end of miR-204, as illustrated in Fig. 4 B.

In vivo model rats. Male rats were injected s.c. with a 60-mg/kg MCT solution (Todorovich-Hunter et al., 1988). PAH was assessed by hemodynamic measurements (using Swan-Gan catheters) and echocardiography (using Vevo 2100; VisualSonics), which were performed as previously described (Bonnet et al., 2007b). In vivo, rats with established PAH (measured by Echo-Doppler) were nebulized with miR-204 mimic (mature sequence, 3′-UUCCCUUUGUCAUCCUAUGCCU-5′) or mimic negative (20 μM once a week for 2 wk). Invivofectamine (Invitrogen) was used as transfected agent according to the manufacturer's instructions. Transfection efficiency and tissue distribution were assessed by qRT-PCR. Tissue distribution was assessed using fluorescent distribution of the commercially available DY547-labeled mimic control (Thermo Fisher Scientific).

Chronic hypoxic mice model. Mice were placed for 2–3 wk in normobaric hypoxic chambers maintained with 5.5–liter min^{-1} flow of hypoxic air (10% O_2 and 90% N_2). Chambers were opened twice a week for cleaning and replenishment of food and water. Oxygen concentration was continuously monitored with blood gas analyzers. Soda lime was used to lower carbon dioxide concentration.

Statistical analysis. Values are expressed as fold change or mean ± SEM. Unpaired Student's *t* tests were used for comparisons between two means. For comparisons between more than two means, we used one-way analysis of variance followed by a Dunn's test. A p-value <0.05 was considered statistically significant (and indicated with asterisks). TLDA and microarray data were analyzed within R (http://www.r-project.org) using the limma package in Bioconductor.

Online supplemental material. Fig. S1 shows seven miRNAs that are aberrantly expressed in human PAH-PASMCs compared with control PASMCs. Fig. S2 represents the measurements of miR-204 level in the pulmonary vasculature and buffy coat. Fig. S3 shows that miR-204 down-regulation in PAH-PASMCs promotes the activation of STAT3 and NFAT. Fig. S4 shows that the miR-204 effect is independent of TRPM3 expression. Fig. S5 shows that the miR-204 mimic molecule restores BMPR2 expression in PAH. Fig. S6 shows that a decrease of miR-204 level activates the Src–STAT3 axis and promotes NFAT expression. Fig. S7 shows that miR-204 mimic intratracheal nebulization restores miR-204 expression in distal PAs, which improves the PAAT and decreases right ventricle hypertrophy in the MCT rat model. Fig. S8 shows the validation of miR-204 mimic/antagomir transfection and siRNA effects on PASMCs. Table S1 lists patients providing tissue. Table S2 lists primers used for ChIP–real-time PCR. Online supplemental material is available at http://www.jem.org/cgi/content/full/jem.20101812/DC1.

This work has been funded by grants from the Canadian Institutes of Health Research (CIHR) to S. Bonnet, M.J. Simard, and J. Côté (MOP-64289). M.J. Simard is a CIHR New Investigator. S. Bonnet and J. Côté hold Canada Research Chairs.

The authors have no conflicting financial interests.

Submitted: 31 August 2010
Accepted: 19 January 2011

REFERENCES

Archer, S., and S. Rich. 2000. Primary pulmonary hypertension: a vascular biology and translational research "Work in progress". *Circulation*. 102:2781–2791.

Banes-Berceli, A.K., P. Ketsawatsomkron, S. Ogbi, B. Patel, D.M. Pollock, and M.B. Marrero. 2007. Angiotensin II and endothelin-1 augment the vascular complications of diabetes via JAK2 activation. *Am. J. Physiol. Heart Circ. Physiol.* 293:H1291–H1299. doi:10.1152/ajpheart.00181.2007

Barman, S.A., S. Zhu, and R.E. White. 2009. RhoA/Rho-kinase signaling: a therapeutic target in pulmonary hypertension. *Vasc. Health Risk Manag.* 5:663–671. doi:10.2147/VHRM.S4711

Barst, R.J. 2005. PDGF signaling in pulmonary arterial hypertension. *J. Clin. Invest.* 115:2691–2694. doi:10.1172/JCI26593

Bonnet, S., and S.L. Archer. 2007. Potassium channel diversity in the pulmonary arteries and pulmonary veins: implications for regulation of the pulmonary vasculature in health and during pulmonary hypertension. *Pharmacol. Ther.* 115:56–69. doi:10.1016/j.pharmthera.2007.03.014

Bonnet, S., E.D. Michelakis, C.J. Porter, M.A. Andrade-Navarro, B. Thébaud, S. Bonnet, A. Haromy, G. Harry, R. Moudgil, M.S. McMurtry, et al. 2006. An abnormal mitochondrial-hypoxia inducible factor-1alpha-Kv channel pathway disrupts oxygen sensing and triggers pulmonary arterial hypertension in fawn hooded rats: similarities to human pulmonary arterial hypertension. *Circulation*. 113:2630–2641. doi:10.1161/CIRCULATIONAHA.105.609008

Bonnet, S., S.L. Archer, J. Allalunis-Turner, A. Haromy, C. Beaulieu, R. Thompson, C.T. Lee, G.D. Lopaschuk, L. Puttagunta, S. Bonnet, et al. 2007a. A mitochondria-K+ channel axis is suppressed in cancer and its normalization promotes apoptosis and inhibits cancer growth. *Cancer Cell*. 11:37–51. doi:10.1016/j.ccr.2006.10.020

Bonnet, S., G. Rochefort, G. Sutendra, S.L. Archer, A. Haromy, L. Webster, K. Hashimoto, S.N. Bonnet, and E.D. Michelakis. 2007b. The nuclear factor of activated T cells in pulmonary arterial hypertension can be therapeutically targeted. *Proc. Natl. Acad. Sci. USA*. 104:11418–11423. doi:10.1073/pnas.0610467104

Bonnet, S., R. Paulin, G. Sutendra, P. Dromparis, M. Roy, K.O. Watson, J. Nagendran, A. Haromy, J.R. Dyck, and E.D. Michelakis. 2009. Dehydroepiandrosterone reverses systemic vascular remodeling through the inhibition of the Akt/GSK3-beta/NFAT axis. *Circulation*. 120:1231–1240. doi:10.1161/CIRCULATIONAHA.109.848911

Bourillot, P.Y., I. Aksoy, V. Schreiber, F. Wianny, H. Schulz, O. Hummel, N. Hubner, and P. Savatier. 2009. Novel STAT3 target genes exert distinct roles in the inhibition of mesoderm and endoderm differentiation in cooperation with Nanog. *Stem Cells*. 27:1760–1771. doi:10.1002/stem.110

Bregeon, J., G. Loirand, P. Pacaud, and M. Rolli-Derkinderen. 2009. Angiotensin II induces RhoA activation through SHP2-dependent dephosphorylation of the RhoGAP p190A in vascular smooth muscle cells. *Am. J. Physiol. Cell Physiol.* 297:C1062–C1070. doi:10.1152/ajpcell.00174.2009

Brock, M., M. Trenkmann, R.E. Gay, B.A. Michel, S. Gay, M. Fischler, S. Ulrich, R. Speich, and L.C. Huber. 2009. Interleukin-6 modulates the expression of the bone morphogenic protein receptor type II through a novel STAT3-microRNA cluster 17/92 pathway. *Circ. Res.* 104:1184–1191. doi:10.1161/CIRCRESAHA.109.197491

Caruso, P., M.R. MacLean, R. Khanin, J. McClure, E. Soon, M. Southgate, R.A. MacDonald, J.A. Greig, K.E. Robertson, R. Masson, et al. 2010. Dynamic changes in lung microRNA profiles during the development of pulmonary hypertension due to chronic hypoxia and monocrotaline.

Arterioscler. Thromb. Vasc. Biol. 30:716–723. doi:10.1161/ATVBAHA.109.202028

Chen, X., H. Xu, P. Yuan, F. Fang, M. Huss, V.B. Vega, E. Wong, Y.L. Orlov, W. Zhang, J. Jiang, et al. 2008. Integration of external signaling pathways with the core transcriptional network in embryonic stem cells. *Cell.* 133:1106–1117. doi:10.1016/j.cell.2008.04.043

Cheranov, S.Y., M. Karpurapu, D. Wang, B. Zhang, R.C. Venema, and G.N. Rao. 2008. An essential role for SRC-activated STAT-3 in 14,15-EET-induced VEGF expression and angiogenesis. *Blood.* 111:5581–5591. doi:10.1182/blood-2007-11-126680

Christman, B.W., C.D. McPherson, J.H. Newman, G.A. King, G.R. Bernard, B.M. Groves, and J.E. Loyd. 1992. An imbalance between the excretion of thromboxane and prostacyclin metabolites in pulmonary hypertension. *N. Engl. J. Med.* 327:70–75. doi:10.1056/NEJM199207093270202

Cowan, K.N., P.L. Jones, and M. Rabinovitch. 2000. Elastase and matrix metalloproteinase inhibitors induce regression, and tenascin-C antisense prevents progression, of vascular disease. *J. Clin. Invest.* 105:21–34. doi:10.1172/JCI6539

Doggrell, S.A. 2005. Rho-kinase inhibitors show promise in pulmonary hypertension. *Expert Opin. Investig. Drugs.* 14:1157–1159. doi:10.1517/13543784.14.9.1157

Dumas de la Roque, E., J.P. Savineau, and S. Bonnet. 2010. Dehydroepiandrosterone: A new treatment for vascular remodeling diseases including pulmonary arterial hypertension. *Pharmacol. Ther.* 126:186–199. doi:10.1016/j.pharmthera.2010.02.003

Dupuis, J., and M.M. Hoeper. 2008. Endothelin receptor antagonists in pulmonary arterial hypertension. *Eur. Respir. J.* 31:407–415. doi:10.1183/09031936.00078207

Ferracin, M., A. Veronese, and M. Negrini. 2010. Micromarkers: miRNAs in cancer diagnosis and prognosis. *Expert Rev. Mol. Diagn.* 10:297–308. doi:10.1586/erm.10.11

Fornaro, M., P.M. Burch, W. Yang, L. Zhang, C.E. Hamilton, J.H. Kim, B.G. Neel, and A.M. Bennett. 2006. SHP-2 activates signaling of the nuclear factor of activated T cells to promote skeletal muscle growth. *J. Cell Biol.* 175:87–97. doi:10.1083/jcb.200602029

Frasch, H.F., C. Marshall, and B.E. Marshall. 1999. Endothelin-1 is elevated in monocrotaline pulmonary hypertension. *Am. J. Physiol.* 276:L304–L310.

Gharavi, N.M., J.A. Alva, K.P. Mouillesseaux, C. Lai, M. Yeh, W. Yeung, J. Johnson, W.L. Szeto, L. Hong, M. Fishbein, et al. 2007. Role of the Jak/STAT pathway in the regulation of interleukin-8 transcription by oxidized phospholipids in vitro and in atherosclerosis in vivo. *J. Biol. Chem.* 282:31460–31468. doi:10.1074/jbc.M704267200

Ghofrani, H.A., W. Seeger, and F. Grimminger. 2005. Imatinib for the treatment of pulmonary arterial hypertension. *N. Engl. J. Med.* 353:1412–1413. doi:10.1056/NEJMc051946

Glazova, M., T.L. Aho, A. Palmetshofer, A. Murashov, M. Scheinin, and P.J. Koskinen. 2005. Pim-1 kinase enhances NFATc activity and neuroendocrine functions in PC12 cells. *Brain Res. Mol. Brain Res.* 138:116–123. doi:10.1016/j.molbrainres.2005.04.003

Humbert, M., G. Monti, F. Brenot, O. Sitbon, A. Portier, L. Grangeot-Keros, P. Duroux, P. Galanaud, G. Simonneau, and D. Emilie. 1995. Increased interleukin-1 and interleukin-6 serum concentrations in severe primary pulmonary hypertension. *Am. J. Respir. Crit. Care Med.* 151:1628–1631.

Humbert, M., N.W. Morrell, S.L. Archer, K.R. Stenmark, M.R. MacLean, I.M. Lang, B.W. Christman, E.K. Weir, O. Eickelberg, N.F. Voelkel, and M. Rabinovitch. 2004. Cellular and molecular pathobiology of pulmonary arterial hypertension. *J. Am. Coll. Cardiol.* 43:S13–S24. doi:10.1016/j.jacc.2004.02.029

Ji, R., Y. Cheng, J. Yue, J. Yang, X. Liu, H. Chen, D.B. Dean, and C. Zhang. 2007. MicroRNA expression signature and antisense-mediated depletion reveal an essential role of MicroRNA in vascular neointimal lesion formation. *Circ. Res.* 100:1579–1588. doi:10.1161/CIRCRESAHA.106.141986

Jurasz, P., D. Courtman, S. Babaie, and D.J. Stewart. 2010. Role of apoptosis in pulmonary hypertension: from experimental models to clinical trials. *Pharmacol. Ther.* 126:1–8. doi:10.1016/j.pharmthera.2009.12.006

Katakami, N., H. Kaneto, H. Hao, Y. Umayahara, Y. Fujitani, K. Sakamoto, S. Gorogawa, T. Yasuda, D. Kawamori, Y. Kajimoto, et al. 2004. Role of pim-1 in smooth muscle cell proliferation. *J. Biol. Chem.* 279:54742–54749. doi:10.1074/jbc.M409140200

Khan, A.A., D. Betel, M.L. Miller, C. Sander, C.S. Leslie, and D.S. Marks. 2009. Transfection of small RNAs globally perturbs gene regulation by endogenous microRNAs. *Nat. Biotechnol.* 27:549–555. doi:10.1038/nbt.1543

Kimura, K., and S. Eguchi. 2009. Angiotensin II type-1 receptor regulates RhoA and Rho-kinase/ROCK activation via multiple mechanisms. Focus on "Angiotensin II induces RhoA activation through SHP2-dependent dephosphorylation of the RhoGAP p190A in vascular smooth muscle cells". *Am. J. Physiol. Cell Physiol.* 297:C1059–C1061. doi:10.1152/ajpcell.00399.2009

Latronico, M.V., and G. Condorelli. 2009. MicroRNAs and cardiac pathology. *Nat Rev Cardiol.* 6:418–429. doi:10.1038/nrcardio.2009.56

Lee, H.H., and Z.F. Chang. 2008. Regulation of RhoA-dependent ROCKII activation by Shp2. *J. Cell Biol.* 181:999–1012. doi:10.1083/jcb.200710187

Lee, Y., X. Yang, Y. Huang, H. Fan, Q. Zhang, Y. Wu, J. Li, R. Hasina, C. Cheng, M.W. Lingen, et al. 2010. Network modeling identifies molecular functions targeted by miR-204 to suppress head and neck tumor metastasis. *PLOS Comput. Biol.* 6:e1000730. doi:10.1371/journal.pcbi.1000730

Li, B., L. Yang, J. Shen, C. Wang, and Z. Jiang. 2007. The antiproliferative effect of sildenafil on pulmonary artery smooth muscle cells is mediated via upregulation of mitogen-activated protein kinase phosphatase-1 and degradation of extracellular signal-regulated kinase 1/2 phosphorylation. *Anesth. Analg.* 105:1034–1041. doi:10.1213/01.ane.0000278736.81133.26

Li, J., X.L. Niu, and N.R. Madamanchi. 2008. Leukocyte antigen-related protein tyrosine phosphatase negatively regulates hydrogen peroxide-induced vascular smooth muscle cell apoptosis. *J. Biol. Chem.* 283:34260–34272. doi:10.1074/jbc.M806087200

Macian, F. 2005. NFAT proteins: key regulators of T-cell development and function. *Nat. Rev. Immunol.* 5:472–484. doi:10.1038/nri1632

McMurtry, M.S., S.L. Archer, D.C. Altieri, S. Bonnet, A. Haromy, G. Harry, S. Bonnet, L. Puttagunta, and E.D. Michelakis. 2005. Gene therapy targeting survivin selectively induces pulmonary vascular apoptosis and reverses pulmonary arterial hypertension. *J. Clin. Invest.* 115:1479–1491. doi:10.1172/JCI23203

Mishra, P.K., N. Tyagi, M. Kumar, and S.C. Tyagi. 2009. MicroRNAs as a therapeutic target for cardiovascular diseases. *J. Cell. Mol. Med.* 13:778–789. doi:10.1111/j.1582-4934.2009.00744.x

Naylor, J., J. Li, C.J. Milligan, F. Zeng, P. Sukumar, B. Hou, A. Sedo, N. Yuldasheva, Y. Majeed, D. Beri, et al. 2010. Pregnenolone sulphate- and cholesterol-regulated TRPM3 channels coupled to vascular smooth muscle secretion and contraction. *Circ. Res.* 106:1507–1515. doi:10.1161/CIRCRESAHA.110.219329

Perros, F., D. Montani, P. Dorfmüller, I. Durand-Gasselin, C. Tcherakian, J. Le Pavec, M. Mazmanian, E. Fadel, S. Mussot, O. Mercier, et al. 2008. Platelet-derived growth factor expression and function in idiopathic pulmonary arterial hypertension. *Am. J. Respir. Crit. Care Med.* 178:81–88. doi:10.1164/rccm.200707-1037OC

Platoshyn, O., V.A. Golovina, C.L. Bailey, A. Limsuwan, S. Krick, M. Juhaszova, J.E. Seiden, L.J. Rubin, and J.X. Yuan. 2000. Sustained membrane depolarization and pulmonary artery smooth muscle cell proliferation. *Am. J. Physiol. Cell Physiol.* 279:C1540–C1549.

Rainio, E.M., J. Sandholm, and P.J. Koskinen. 2002. Cutting edge: Transcriptional activity of NFATc1 is enhanced by the Pim-1 kinase. *J. Immunol.* 168:1524–1527.

Rajkumar, R., K. Konishi, T.J. Richards, D.C. Ishizawar, A.C. Wiechert, N. Kaminski, and F. Ahmad. 2010. Genomewide RNA expression profiling in lung identifies distinct signatures in idiopathic pulmonary arterial hypertension and secondary pulmonary hypertension. *Am. J. Physiol. Heart Circ. Physiol.* 298:H1235–H1248. doi:10.1152/ajpheart.00254.2009

Sakao, S., L. Taraseviciene-Stewart, J.D. Lee, K. Wood, C.D. Cool, and N.F. Voelkel. 2005. Initial apoptosis is followed by increased proliferation of apoptosis-resistant endothelial cells. *FASEB J.* 19:1178–1180.

Sato, K., T. Nagao, M. Kakumoto, M. Kimoto, T. Otsuki, T. Iwasaki, A.A. Tokmakov, K. Owada, and Y. Fukami. 2002. Adaptor protein Shc is an isoform-specific direct activator of the tyrosine kinase c-Src. *J. Biol. Chem.* 277:29568–29576. doi:10.1074/jbc.M203179200

Shibata, R., H. Kai, Y. Seki, S. Kato, Y. Wada, Y. Hanakawa, K. Hashimoto, A. Yoshimura, and T. Imaizumi. 2003. Inhibition of STAT3 prevents neointima formation by inhibiting proliferation and promoting apoptosis of neointimal smooth muscle cells. *Hum. Gene Ther.* 14:601–610. doi:10.1089/104303403321618128

Steiner, M.K., O.L. Syrkina, N. Kolliputi, E.J. Mark, C.A. Hales, and A.B. Waxman. 2009. Interleukin-6 overexpression induces pulmonary hypertension. *Circ. Res.* 104:236–244. doi:10.1161/CIRCRESAHA.108.182014

Steudel, W., F. Ichinose, P.L. Huang, W.E. Hurford, R.C. Jones, J.A. Bevan, M.C. Fishman, and W.M. Zapol. 1997. Pulmonary vasoconstriction and hypertension in mice with targeted disruption of the endothelial nitric oxide synthase (NOS 3) gene. *Circ. Res.* 81:34–41.

Stewart, D.J., R.D. Levy, P. Cernacek, and D. Langleben. 1991. Increased plasma endothelin-1 in pulmonary hypertension: marker or mediator of disease? *Ann. Intern. Med.* 114:464–469.

Tada, Y., S. Majka, M. Carr, J. Harral, D. Crona, T. Kuriyama, and J. West. 2007. Molecular effects of loss of BMPR2 signaling in smooth muscle in a transgenic mouse model of PAH. *Am. J. Physiol. Lung Cell. Mol. Physiol.* 292:L1556–L1563. doi:10.1152/ajplung.00305.2006

Todorovich-Hunter, L., D.J. Johnson, P. Ranger, F.W. Keeley, and M. Rabinovitch. 1988. Altered elastin and collagen synthesis associated with progressive pulmonary hypertension induced by monocrotaline. A biochemical and ultrastructural study. *Lab. Invest.* 58:184–195.

Tuder, R.M., J.C. Marecki, A. Richter, I. Fijalkowska, and S. Flores. 2007. Pathology of pulmonary hypertension. *Clin. Chest Med.* 28:23–42: vii. doi:10.1016/j.ccm.2006.11.010

Wang, F.E., C. Zhang, A. Maminishkis, L. Dong, C. Zhi, R. Li, J. Zhao, V. Majerciak, A.B. Gaur, S. Chen, and S.S. Miller. 2010. MicroRNA-204/211 alters epithelial physiology. *FASEB J.* 24:1552–1571. doi:10.1096/fj.08-125856

Wang, L., D. Xu, W. Dai, and L. Lu. 1999. An ultraviolet-activated K+ channel mediates apoptosis of myeloblastic leukemia cells. *J. Biol. Chem.* 274:3678–3685. doi:10.1074/jbc.274.6.3678

Wong, W.K., J.A. Knowles, and J.H. Morse. 2005. Bone morphogenetic protein receptor type II C-terminus interacts with c-Src: implication for a role in pulmonary arterial hypertension. *Am. J. Respir. Cell Mol. Biol.* 33:438–446. doi:10.1165/rcmb.2005-0103OC

Wu, J.H., R. Goswami, X. Cai, S.T. Exum, X. Huang, L. Zhang, L. Brian, R.T. Premont, K. Peppel, and N.J. Freedman. 2006. Regulation of the platelet-derived growth factor receptor-beta by G protein-coupled receptor kinase-5 in vascular smooth muscle cells involves the phosphatase Shp2. *J. Biol. Chem.* 281:37758–37772. doi:10.1074/jbc.M605756200

Yellaturu, C.R., and G.N. Rao. 2003. Cytosolic phospholipase A2 is an effector of Jak/STAT signaling and is involved in platelet-derived growth factor BB-induced growth in vascular smooth muscle cells. *J. Biol. Chem.* 278:9986–9992. doi:10.1074/jbc.M211276200

Yildiz, P. 2009. Molecular mechanisms of pulmonary hypertension. *Clin. Chim. Acta.* 403:9–16. doi:10.1016/j.cca.2009.01.018

Yu, Y., M. Sweeney, S. Zhang, O. Platoshyn, J. Landsberg, A. Rothman, and J.X. Yuan. 2003. PDGF stimulates pulmonary vascular smooth muscle cell proliferation by upregulating TRPC6 expression. *Am. J. Physiol. Cell Physiol.* 284:C316–C330.

Yu, Y., I. Fantozzi, C.V. Remillard, J.W. Landsberg, N. Kunichika, O. Platoshyn, D.D. Tigno, P.A. Thistlethwaite, L.J. Rubin, and J.X. Yuan. 2004. Enhanced expression of transient receptor potential channels in idiopathic pulmonary arterial hypertension. *Proc. Natl. Acad. Sci. USA.* 101:13861–13866. doi:10.1073/pnas.0405908101

Yuan, X.J. 1995. Voltage-gated K+ currents regulate resting membrane potential and [Ca2+]i in pulmonary arterial myocytes. *Circ. Res.* 77:370–378.

Zakrzewicz, A., M. Hecker, L.M. Marsh, G. Kwapiszewska, B. Nejman, L. Long, W. Seeger, R.T. Schermuly, N.W. Morrell, R.E. Morty, and O. Eickelberg. 2007. Receptor for activated C-kinase 1, a novel interaction partner of type II bone morphogenetic protein receptor, regulates smooth muscle cell proliferation in pulmonary arterial hypertension. *Circulation.* 115:2957–2968. doi:10.1161/CIRCULATIONAHA.106.670026

Zhang, C. 2009. MicroRNA-145 in vascular smooth muscle cell biology: a new therapeutic target for vascular disease. *Cell Cycle.* 8:3469–3473. doi:10.4161/cc.8.21.9837

Zhao, L., R. al-Tubuly, A. Sebkhi, A.A. Owji, D.J. Nunez, and M.R. Wilkins. 1996. Angiotensin II receptor expression and inhibition in the chronically hypoxic rat lung. *Br. J. Pharmacol.* 119:1217–1222.